

Exposing Sgr tidal debris behind the Galactic disk with M giants selected in WISE \cap 2MASS

S. E. Koposov¹*, V. Belokurov¹, D. B. Zucker^{2,3,4}, G. F. Lewis⁵, R. A. Ibata⁶,
E. W. Olszewski⁷, Á. R. López-Sánchez^{4,3}, E. A. Hyde^{2,3}

¹*Institute of Astronomy, Madingley Rd, Cambridge, CB3 0HA, UK*

²*Macquarie University Research Centre in Astronomy, Astrophysics & Astrophotonics, NSW 2109, Australia*

³*Department of Physics and Astronomy, Macquarie University, North Ryde, NSW 2109, Australia*

⁴*Australian Astronomical Observatory, PO Box 915, North Ryde, NSW 1670, Australia*

⁵*Sydney Institute for Astronomy, School of Physics, A28, University of Sydney, Sydney NSW 2006, Australia*

⁶*Observatoire Astronomique de Strasbourg, Université de Strasbourg, CNRS, UMR 7550, 11 rue de l'Université, F-67000 Strasbourg, France*

⁷*Steward Observatory, University of Arizona, Tucson, AZ 85721, USA*

7 September 2018

ABSTRACT

We show that a combination of infrared photometry from WISE and 2MASS surveys can yield highly pure samples of M giant stars. We take advantage of the new WISE \cap 2MASS M giant selection to trace the Sagittarius trailing tail behind the Galactic disk in the direction of the anti-centre. The M giant candidates selected via broad-band photometry are confirmed spectroscopically using AAOmega on the AAT in 3 fields around the extremity of the Sgr trailing tail in the Southern Galactic hemisphere. We demonstrate that at the Sgr longitude $\tilde{\Lambda}_{\odot} = 204^{\circ}$, the line-of-sight velocity of the trailing tail starts to deviate from the track of the Law & Majewski (2010) model, confirming the prediction of Belokurov et al. (2014). This discovery serves to substantiate the measurement of low differential orbital precession of the Sgr stream which in turn may imply diminished dark matter content within 100 kpc.

1 INTRODUCTION

Across the Milky Way, the safest place to conceal the remains of a destroyed satellite is behind the Galactic disk. This is exactly where the third largest, and the closest, companion galaxy, the Sagittarius dwarf, avoided discovery until the end of the last millennium (Ibata et al. 1994). In the twenty years that followed, through the meticulous identification of particular stellar tracers, Sagittarius's enormous tidal tails have been shown to wrap around the entire Milky Way (Mateo et al. 1996; Totten & Irwin 1998; Mateo et al. 1998; Majewski et al. 1999; Ivezić et al. 2000; Yanny et al. 2000; Ibata et al. 2001; Martínez-Delgado et al. 2001; Vivas et al. 2001; Dohm-Palmer et al. 2001; Newberg et al. 2002, 2003; Majewski et al. 2003; Belokurov et al. 2006; Yanny et al. 2009; Niederste-Ostholt et al. 2010; Correnti et al. 2010; Ruhlmann et al. 2011; Koposov et al. 2012; Belokurov et al. 2014). Yet, after two decades of collaborative effort, two minute gaps are still present: close to the Galactic plane, no choice of stellar tracer results in a selection clean enough not to be completely swamped by the nearby disk dwarfs. As a result, in the direction towards the bulge, the base of the leading tail is lacking, while in the opposite direction, towards the Galactic anti-centre, the sight of the trailing debris is lost as it reaches into the disk from below the plane.

These short (at most 20–30 degrees on the sky) missing stream pieces, nevertheless, hold tantalising clues to the disruption of the Sagittarius dwarf (Sgr). If it were not obscured by the disk and the bulge, the view of the area where the leading tail attaches to

the remnant's body could help explain the peculiar stream bifurcation. As pointed out by Belokurov et al. (2006), the leading tail appears bifurcated into the bright and faint components. As of today, no convincing mechanism has been found to produce such splitting of the Sgr tidal tails. Several hypotheses have been brought up: i) a group or binary in-fall (e.g. Helmi et al. 2011; Koposov et al. 2012), and ii) a rotating progenitor (Peñarrubia et al. 2010, 2011). Each of these scenarios predicts distinctly different behaviour of the leading tail(s) in the vicinity of the progenitor.

Similarly, as pointed out by Belokurov et al. (2014), the exact distance and velocity of the trailing debris around the Galactic anti-centre can be used to understand the Sgr stream's precession. They identify new far-flung tidal debris coincident with Sgr's orbital plane in the Northern hemisphere, and argue that, having crossed the Milky Way's disk, the trailing tail reaches much larger distances than expected. In so doing, it attains its maximal extent, or apo-centre, later than predicted by most current models, yielding, therefore, a smaller orbital precession angle. The larger apo-centric distance and the smaller differential precession point towards a significantly lower dark matter content within the stream's orbit, as has been recently demonstrated by Gibbons et al. (2014). However, Belokurov et al. (2014) based their inference on the assumption that the distant stream detected above the disk in the North is simply the continuation of Sgr's Southern trailing tail. While this conjecture might seem reasonable, as both streams separated by the Galactic disk follow very similar distance and velocity gradients, it

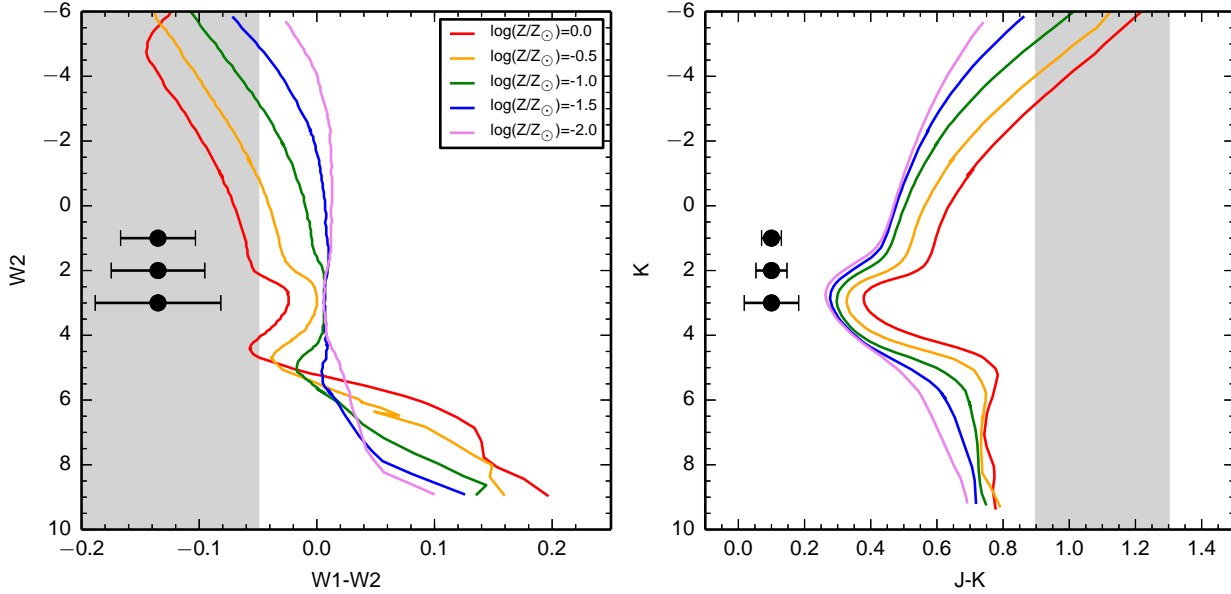


Figure 1. PARSEC isochrones for an old stellar population with five different metallicities in infrared pass-bands. *Left:* Isochrones in WISE W1, W2 bands. *Right:* Isochrones in 2MASS J,K filters. Note the change in the behaviour of the metal-rich RGB stars: while being red in the near-IR (and optical), these are blue in the WISE colours. Grey shows the colour range used for the M giant selection proposed here. The horizontal error-bars show the approximate photometric errors expected for the colours of an M giant with absolute magnitude in $M_{W2} \sim 5$ at distances of 20, 40 and 60 kpc.

is at odds with established models of Sgr’s disruption (see, e.g., Law & Majewski 2010).

The most tangible difference between the two pictures of Sgr trailing arm behaviour around the Galactic anti-centre is apparent in Figure 11 of Belokurov et al. (2014). This shows the evolution of the line-of-sight velocities of the Sgr tails as a function of the Sgr longitude, $\hat{\Lambda}_{\odot}$. While at most longitudes the data and the model are in good agreement, the larger apocentric distance of 100 kpc observed by Belokurov et al. (2014) implies that, on approach to the Galactic disk, the Sgr trailing tail should deviate significantly from the model of Law & Majewski (2010). Namely, the radial velocity of the trailing debris is predicted to be appreciably faster (higher negative velocity) than that of the model. Thus the key test of the Belokurov et al. (2014) conjecture is the measurement of the stream’s line-of-sight velocities near the Galactic plane, where the stream stars return from the apocenter. In Sgr stream coordinates, the region of interest is around $\hat{\Lambda}_{\odot} \sim 200$, which corresponds to a rather low Galactic latitude $|b| \lesssim 20^{\circ}$.

Previously, a wide variety of stellar types have been used to trace Sgr tidal debris. For example, main sequence (MS) and main sequence turn-off (MSTO) stars are the most numerous amongst the Sgr populations, and have been used with great success to chart the position of the tails on the sky (e.g. Koposov et al. 2012). However, at distances beyond 30 kpc, these are too faint for spectroscopic follow-up. While blue horizontal branch (BHB) stars are perfect distance indicators, their density in this part of the trailing tail is surprisingly low (see Koposov et al. 2012); more importantly, in the vicinity of the Galactic disk, the efficiency of BHB identification quickly deteriorates with mounting dust reddening. Red giants are bright spectroscopic targets, but even at high latitudes photometrically selected candidates are dominated by the thick disk dwarfs. Therefore, their follow-up close to the Milky Way’s plane appears impractical. The two remaining tracers that might withstand significant levels of disk dwarf contamination include RR Lyrae and

M giants. RR Lyrae stand apart from any other stellar population due to their characteristic variability. For instance, the OGLE survey has produced multi-epoch datasets in which RR Lyrae are routinely detected beyond the bulge and the disk at latitudes as low as $|b| \sim 2^{\circ}$ (see e.g. Pietrukowicz et al. 2012). Unfortunately, the region of interest around the Galactic anti-centre has not been surveyed with sufficient temporal resolution and depth to identify RR Lyrae in the Sgr stream.

Taking advantage of the full-sky coverage of the 2MASS survey (Skrutskie et al. 2006), Ibata et al. (2002) and Majewski et al. (2003) applied the infrared selection criteria outlined by Bessell & Brett (1988) to pick out distant halo M giants. As these studies demonstrate, at high latitudes and distances beyond 20 kpc, Sgr debris dominates the M giant counts. This ought to be caused by a combination of three distinct effects: the typical lifetime of an M giant star, the star-formation history of Sgr and the paucity of recent massive dwarf galaxy accretion onto the Milky Way. It turns out that, within 30–40 kpc from the Sun, the M giant selection based on 2MASS JHK magnitudes can distinguish giants from dwarfs quite efficiently, even at Galactic latitudes as low as $|b| \sim 20^{\circ}$, as illustrated by the discovery of the debris from an accretion event passing through the constellations of Triangulum and Andromeda (Rocha-Pinto et al. 2004). However, for fainter stars and/or objects closer to the Galactic plane, M giant selection based on 2MASS photometry starts to falter. Therefore, to be able to proceed with the kinematic study of the Sgr trailing tail around the anti-centre, we strive to optimise M giant identification by complementing the 2MASS photometry with far-infrared data from the WISE survey (Wright et al. 2010). Section 2 gives the details of the proposed tracer selection, while Section 3 presents the results of the spectroscopic follow-up of the Sgr M giant candidate stars.

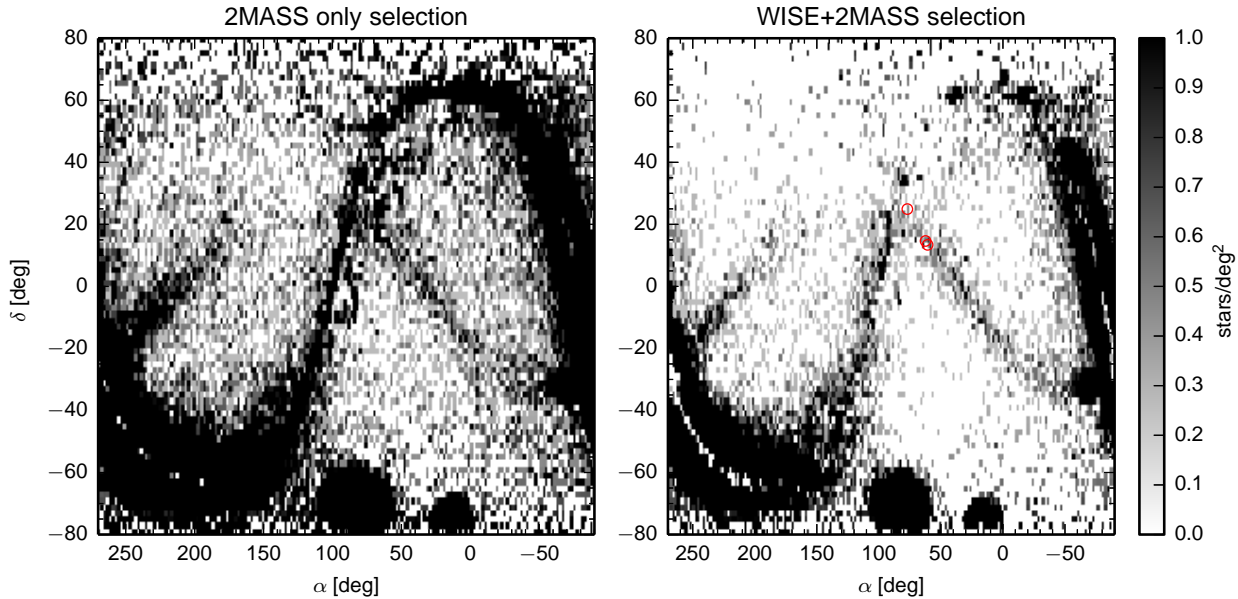


Figure 2. *Left:* Density map of the M giant stars selected using 2MASS photometry only, i.e. $0.9 < J - K < 1.3$, $0.22 < J - H - 0.561 (J - K) < 0.46$ and $11 < K < 13$ (see also Majewski et al. 2003). *Right:* Density map of the M giants selected using WISE \cap 2MASS: $0.9 < J - K < 1.3$, $-0.2 < W1 - W2 < -0.05$ and $11 < K < 13$. Note the cleaner M giant selection provided by the combination of WISE and 2MASS, at both low and high Galactic latitudes. The locations of three fields targeted with AAOmega spectroscopy are indicated with open red circles.

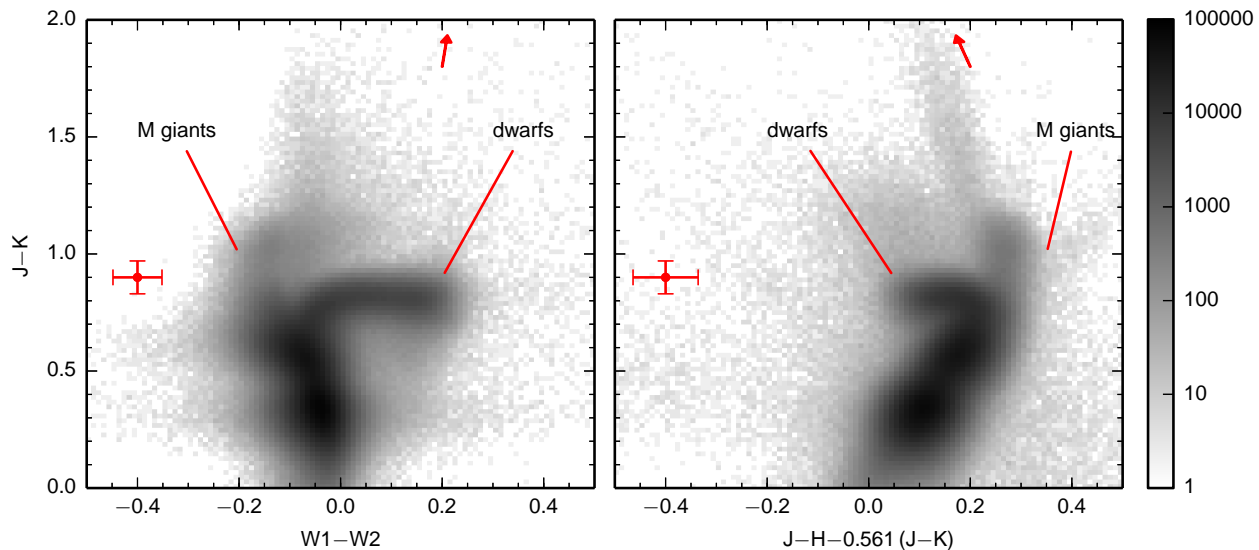


Figure 3. Stellar density distribution in near-IR and IR colour-colour spaces. *Left:* Positions of stars with $J \sim 13$ and $|b| > 10$ in the $(W1-W2, J-K)$ plane. The dwarf and giant sequences start to separate at $W1-W2 \sim -0.1$ and $J-K \sim 0.8$. *Right:* The same stars are now plotted in the $(J-H-0.561(J-K), J-K)$ space. The X-axis of this panel is the colour combination used for M giant selection by Majewski et al. (2003). In both panels, small arrows show the direction of the dust extinction, while the error-bars illustrate the characteristic photometric uncertainty for an M-giant with a magnitude of $J \sim 14$. In the WISE bands, the bulk of metal-rich M giants (at negative $W1-W2$) is further away from the dwarf population as compared to the 2MASS JHK color combination (at similar $J-K$ color). We argue that, at faint magnitudes, this leads to noticeably cleaner samples of M giants.

2 M GIANT SELECTION WITH WISE \cap 2MASS

Figure 3 of Majewski et al. (2003) exemplifies the power of infrared-based M giant selection: this was the very first time the immense scale of Sgr’s disruption was shown in such clarity. However, in this Figure the contamination of the M giant sample at low latitudes is already obvious, even though the most affected ar-

eas with $|b| \lesssim 15^\circ$ have been excised. It is clear that the original identification scheme breaks down at i) large distances and ii) high reddening as the limits of the 2MASS photometry are approached. Additionally, next to the Milky Way plane, the number of false positives due to disk dwarfs grows overwhelmingly quickly making a spectroscopic follow-up campaign too costly. Below we show that

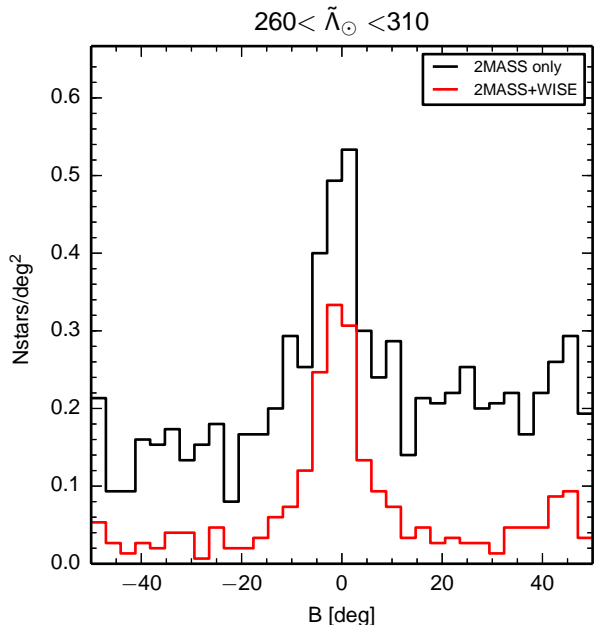


Figure 4. Density profiles of the Sgr trailing tail in the range $260^\circ < \tilde{\Lambda}_\odot < 310^\circ$ as traced by M giants selected using 2MASS only (black) and WISE \cap 2MASS (red). While the stream signal remains largely the same in both profiles, the foreground contamination appears dramatically reduced when WISE \cap 2MASS is employed.

these problems can be remedied if, for selecting Sgr stream M giants, 2MASS data are used in conjunction with far-infrared photometry from the WISE survey.

Intriguingly, the WISE data turn out to be extremely valuable for the particular task of identifying giant stars. The information gain here is due to the peculiar behaviour of the mid-infrared colours of metal-rich giants. Optical and near-infrared broad-band colours of giant stars are quite similar to those of dwarfs, making giant tracer selection rather inefficient. Conversely, in WISE photometry, metal-rich giants stand out from dwarfs thanks to the presence of the gravity-sensitive CO-bands. Unusually, this makes the metal-rich giants *bluer* in $W1-W2$ colours compared to dwarf stars!

Figure 1 illustrates this effect. Here, five 12 Gyr PARSEC (Bressan et al. 2012) isochrones with different metallicities are shown. The near-IR isochrones look as usual, i.e., the metal-rich tracks are redder than metal-poor tracks. Moreover, both giants and dwarfs are also redder compared to the turnoff stars. However, along mid-IR isochrones, the metal-rich giant branch actually turns blue in the $W1-W2$ colour, which would clearly make the M giants stand out further from the dwarfs. This behaviour of the mid-IR giant tracks points out the route for their efficient selection: we need stars that are red in the 2MASS bands, $(J-K) \gtrsim 0.9$, and blue in the WISE bands, $W1-W2 \lesssim -0.05$. Additionally, Figure 1 shows the expected median photometric uncertainty for an M-giant with $M_{W2} = 5$ placed at heliocentric distances of 20, 40 and 60 kpc. This demonstrates how the photometric accuracy deteriorates as stars at larger distances are selected. As far as distant halo tracers or areas with large levels of extinction are concerned, the efficiency of this giant identification is limited by the quality of the WISE photometry. At around $W1 \sim 14$, the WISE photometric errors become large enough that the candidate tracers are swamped by the dwarf stars with $W1-W2 \gtrsim 0$.

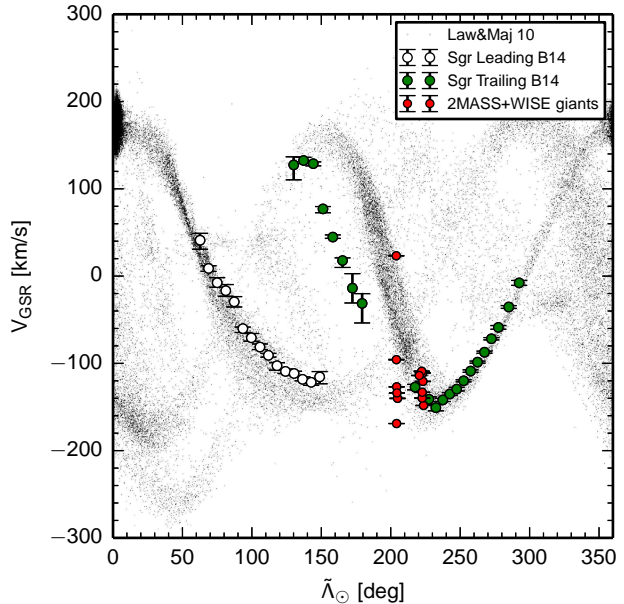


Figure 6. Galactocentric radial velocities of the Sgr tidal debris as a function of the angle along the stream. Small black dots show the phase-space positions of the N-body particles in the Law & Majewski (2010) model. Green and unfilled circles with error-bars are the compilation of the available kinematic data for the trailing and leading tail, respectively, from Belokurov et al. (2014). Filled red circles show the new M giant radial velocities reported in this work. Note that our data agree with the literature values at $\tilde{\Lambda}_\odot \sim 220^\circ$. However, closer to the disk, at $\tilde{\Lambda}_\odot = 204^\circ$, we show that the trailing tail is at lower velocity than predicted by the Law & Majewski (2010) model. This finding supports the hypothesis of Belokurov et al. (2014) as to the properties of the trailing tail in the Northern hemisphere.

Figure 2 demonstrates the improvement in the quality of the M giant selection. It compares two all-sky density maps: one (left panel) obtained by applying the original 2MASS selection as proposed by Majewski et al. (2003), and another (right panel) built using the following combination of WISE and 2MASS:

$$\begin{aligned} -0.2 < (W1 - W2)_0 < -0.05 \\ 11 < W1_0 < 13.5 \\ 0.9 < (J - K)_{2MASS,0} < 1.3 \end{aligned} \quad (1)$$

Here, all magnitudes are corrected for extinction using the maps provided by Schlegel et al. (1998).

The two density distributions have features in common. For example, the leading ($100^\circ < \alpha < 260^\circ$) as well as the trailing tail ($-60^\circ < \alpha < 80^\circ$) of the Sgr stream, are equally prominent in both maps, although perhaps in the right panel there is a minor depletion in M giant counts in the most distant part of the leading tail, where WISE photometry starts to deteriorate. However, there are more important differences too. The halo, i.e., the portions of the sky far away from the Galactic disk, appears both tidier and emptier with the new selection. Also, there is a lot less junk close to the disk, while the disk itself appears significantly reduced in density, especially around the anti-centre - the region of interest ($\alpha \sim 100^\circ$). In addition, it is worth noting that the new WISE \cap 2MASS M giant map also boasts a clearer view of the

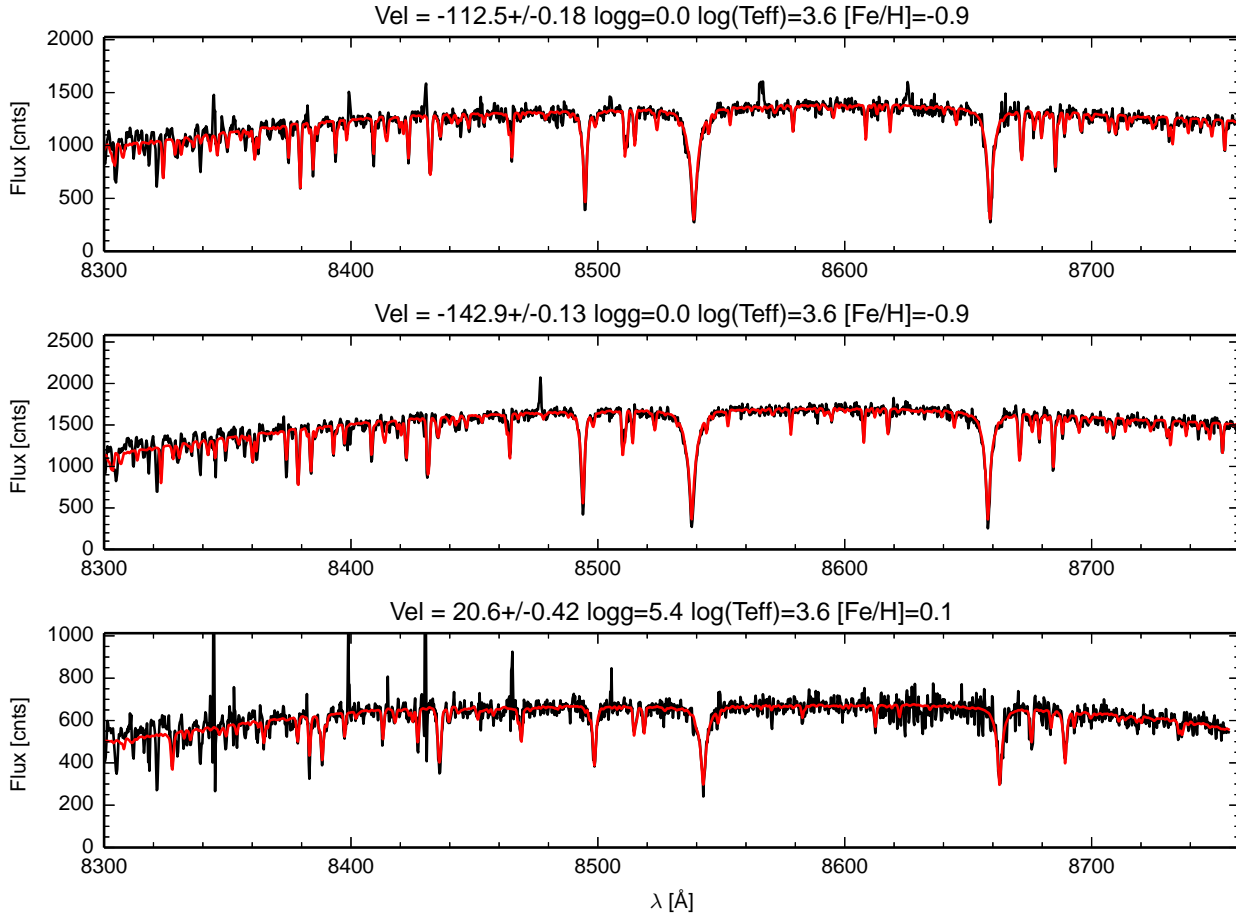


Figure 5. Sample AAOmega spectra of three of our M giant candidates. Black shows the data, red lines show the best-fit model templates. The spectra in the top and middle panels correspond to Sgr stars while the bottom spectrum is a foreground dwarf star.

Triangulum-Andromeda merger (or Tri-And, see Deason et al 2014 for details) at $-20^\circ \lesssim \alpha \lesssim 80^\circ$ and $10^\circ \lesssim \delta \lesssim 50^\circ$.

Figure 4 gives a more quantitative summary of the efficiency of the new selection. The Figure presents two density profiles of the same piece of the Sgr trailing tail with $260^\circ < \tilde{\Lambda}_\odot < 310^\circ$: one produced using 2MASS only (black), and one employing the WISE \cap 2MASS selections (red). As demonstrated here, the amplitude of the stream detection remains largely unchanged when switching to WISE \cap 2MASS, while the foreground contamination is significantly reduced. By fitting the Gaussian model together with the linearly changing foreground density to both datasets we find that the efficiency of selecting Sgr M-giant stars using WISE \cap 2MASS is within 10% of the efficiency of the 2MASS-only selection, while the contamination is ~ 6 times lower for this particular area of the sky. Overall, given the performance of the new M giant selection for the detection of previously identified stellar halo sub-structures, we conclude that the WISE photometry indeed helps to reduce the contamination levels appreciably.

Given that the quality of any “colour-cut” selection method is a complicated function of i) the distribution of the sources of interest in colour-space, ii) the distribution of their contaminants, as well as iii) the photometric errors and iv) extinction coefficients, it is not straightforward to pinpoint one factor responsible for the increased efficiency of the proposed WISE \cap 2MASS selection. Nonetheless, Figure 3 provides a further exposition as to why the WISE photom-

Table 1. Location of the 2dF fields

Field	$\tilde{\Lambda}_\odot$ deg	\tilde{B}_\odot deg	α deg	δ deg	l deg	b deg
1	204.2	2.7	77.1	24.8	178.8	-9.2
2	221.0	-1.0	62.4	14.6	178.2	-26.4
3	223.0	-1.4	60.6	13.3	178.0	-28.5

etry might be of help. This Figure compares the behaviour of stellar loci in the $(W1 - W2, J - K)$ space to that in $(J - H - 0.561(J - K), J - K)$, the space originally used by Majewski et al. (2003). We argue, that due to the peculiar behaviour of the WISE colours of the metal-rich giants, these stars tend to be further apart from the bulk of the dwarfs (their main contaminants) at similar $J - K$ colour. Furthermore, as illustrated by the error-bars over-plotted, at fainter magnitudes $J \sim 14$, the 2MASS-only selection is more affected by photometric errors. This photometric deterioration is exacerbated in the presence of significant extinction; the 2MASS-only selections will suffer a more pronounced loss due to larger extinction coefficients.

Table 2. Kinematic and photometric properties of M giant candidates

ID	Field	α deg	δ deg	V_{GSR} km s ⁻¹	σ_V km s ⁻¹	W1 mag	W2 mag	J(2MASS) mag	K(2MASS) mag	log(g) dex
0	1	77.3832	24.7543	15.3	0.4	13.43	13.47	14.65	13.49	5.4
1	1	77.0267	24.75	-126.9	0.2	13.15	13.23	14.64	13.34	0
2	1	76.5295	24.2549	-140.1	0.3	12.75	12.83	14.08	12.82	0
3	1	76.5367	25.3871	-133.9	0.3	12.35	12.41	14.1	12.57	0
4	1	77.0282	24.9731	-169	0	11.63	11.75	13.26	11.95	0
5	1	77.0944	25.6639	-112.5	1	13.65	13.79	15.2	13.82	5.6
6	1	77.1975	25.1967	23.3	0.2	11.57	11.68	12.93	11.7	0
7	1	77.1774	25.0204	-95.8	0.3	13.21	13.27	14.47	13.27	0
8	2	61.1325	13.2303	0.4	0.3	13.08	13.14	14.3	13.2	5.5
9	2	60.4733	12.4608	-148.3	0.1	11.78	11.83	13.1	11.91	0
10	2	60.2445	13.874	-120.7	0.2	12.61	12.69	13.86	12.66	0
11	2	60.5928	13.5688	-110.9	0.3	13.5	13.56	14.88	13.77	0
12	2	61.1166	14.1835	-109.1	0.3	13.35	13.44	14.66	13.43	0
13	2	61.0215	13.6043	-139.8	0.1	11.89	11.94	13.16	12.09	0
14	2	61.0472	13.4434	-133.2	0.2	12.22	12.28	13.52	12.45	0
15	3	62.5388	15.3289	-113.9	0.2	12.38	12.44	13.83	12.58	0

3 KINEMATICS OF THE SGR TRAILING TAIL AROUND THE ANTI-CENTRE

We used the newly devised method of M giant identification, as described in the previous section, to pick out targets for a spectroscopic follow-up program. To measure the line-of-sight velocities of Sgr debris, 2dF+AAOmega on Anglo-Australian Telescope (AAT) was used to target 3 locations along the trailing tail.¹ The exact coordinates were chosen according to a small number of simple rules. First, two validation fields (Fields 2 and 3) were selected, i.e., locations where Sgr debris has been previously studied with spectroscopy. Second, a field (Field 1) as far away along the trailing tail from the last known debris detection was identified. When placing the fields we attempted to locate them in such a way as to maximise the number of M giant star candidates in the 2dF field of view as well as to avoid very extinguished patches of the sky. The coordinates of all three pointings are listed in Table 1. To fill all the AAOmega fibers, the WISE \cap 2MASS M giant candidate sample was complemented by additional objects having colours and magnitudes consistent with the red giant branch stars at distances $30 \lesssim R_{hel} \lesssim 100$ kpc. Note that one of the fields was selected to lie within the UKIDSS GCS (Lawrence et al. 2007) survey footprint, hence we used UKIDSS J, K photometry instead of 2MASS. To summarise, Field 1 had 8 M giant candidates allocated, Field 2 had 7, and, finally, Field 3 had only 1 WISE \cap 2MASS M giant candidate, yielding a total of 16 across all 3 fields.

The designated three fields in the Sgr Stream near $l, b = (180, -20)$ were observed with the 2dF top end + AAOmega spectrograph on the 3.9m Anglo-Australian Telescope the night of 27 November, 2013, as part of service programme AO179. 2dF is a robotic positioner which allocates up to 392 2'' fibres to targets across a 2° diameter field of view. These fibres feed AAOmega's blue and red arms simultaneously, which for our observations were configured with 580V and 1700D gratings for central wavelengths / resolutions of 4800Å / 1300 and 8540Å / 8000, respectively. Each field was observed for 3×1800 s, at airmasses ranging from $\sim 1.4 - 2$ and typical seeing of $\sim 2.5''$, with quartz spectroscopic fibre

flat fields and arc lamp spectra taken immediately prior to each set of exposures. We processed both blue and red camera data using version 5.53 of the 2dfdr reduction pipeline, although in this work we consider only the red spectra, i.e., those centred on the Ca II infrared triplet.

Following the approach described in detail in Koposov et al. (2011), the reduced spectra were then analyzed to determine the best-fit stellar template, chosen from the PHOENIX grid (see Husser et al. 2013), whilst simultaneously measuring line-of-sight velocities. All objects with the best-fit $\log(g) < 2$ were classified as giants. Among the 16 stars targeted as M giant candidates, 13 had $\log(g) < 2$ (6 from Field 1, 6 from Field 2 and 1 from Field 3). Example spectra of three of the observed stars are shown in Figure 5 together with their best fitting models. According to the results of our fitting procedure, of these three, two are giants (top and middle) and one is a dwarf (bottom). Notwithstanding the relatively small sample size, our spectroscopic follow-up program confirms the high efficiency (in excess of 80%) of the WISE \cap 2MASS M giant selection method.

Figure 6 gives the summary of all M giants with measured radial velocities (corrected for the solar motion) in our AAOmega spectroscopic sample (red circles) as a function of the angle along the stream, $\tilde{\Lambda}_{\odot}$. The Figure also shows previous measurements of the line-of-sight velocities of the leading (empty circles) and the trailing (green circles) tails as well as the prediction from the model of Law & Majewski (2010) (black dots). Reassuringly, the radial velocities of the Sgr trailing tail in the two validation fields (at around $\tilde{\Lambda}_{\odot} \sim 220^\circ$) match well the values from the literature. Stepping farther from the progenitor along the trailing tail, Field 1 at $\tilde{\Lambda}_{\odot} \sim 204^\circ$ shows a clear deviation from the kinematics stipulated by the N-body simulation. Here, 5 out of 6 confirmed M giants are at lower radial velocities, following the trend suggested by Belokurov et al. (2014). The sixth M giant star has $V_{GSR} \sim 20$ km s⁻¹. We surmise that this is unlikely to be a dwarf interloper (even though this field is at a lower Galactic latitude than the other two) but rather a member of the Tri-And structure (see the recent studies of Deason et al. 2014; Sheffield et al. 2014).

Interestingly, the radial velocities of M giants in the Sgr stream show an appreciable scatter. This is not likely to be caused by the contamination or the accuracy of our velocity measurements but

¹ We originally planned to observe 5 fields extending all the way to the disk plane, however only 3 were eventually observed.

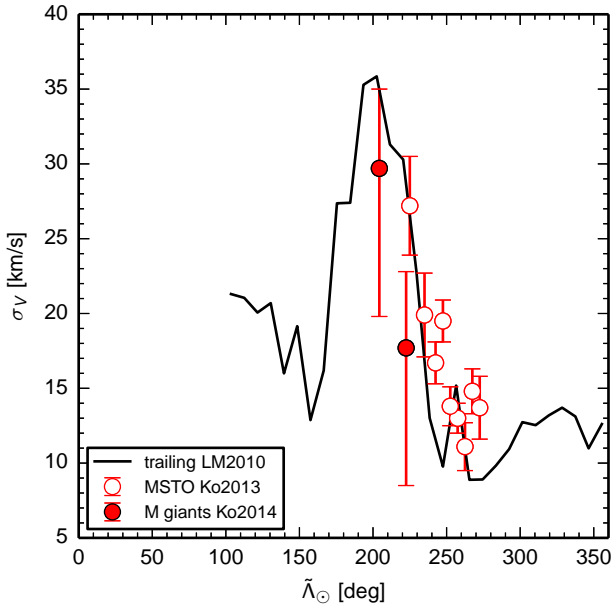


Figure 7. The velocity dispersion of the Sgr Stream trailing tail as measured by M giants (filled points), MSTO stars from Koposov et al. (2013) (empty circles) and compared with the predictions of the Law & Majewski model (black solid line).

rather by the behaviour of the tidal stream around the turn-around in the phase space. A similar trend of increasing stream dispersion was in fact observed before, for example in Koposov et al. (2013). This is, of course, also predicted by Sgr disruption models in general and the Law & Majewski model in particular. Figure 7 shows how the velocity dispersion that we derive from M giants compares to the prediction of the Law & Majewski model as well with the measurements by Koposov et al. (2013). The M giant velocity dispersion presented here matches within the error-bars the trend of growing trailing tail velocity dispersion around $\tilde{\lambda}_{\odot} = 200^{\circ}$.

4 CONCLUSIONS

We have presented a new method to identify M giant stars using broad-band infrared photometry, more precisely a combination of 2MASS and WISE data. Our selection procedure picks out stars that are red in the near-infrared $J-K$ colour and blue in the mid-infrared $W1-W2$ colour. Thanks to the presence of the gravity sensitive CO bands in WISE (leading to a larger colour separation of dwarfs and giants), the resulting WISE \cap 2MASS sample of M giants suffers significantly less contamination (up to a factor of 6) from foreground dwarfs compared to the conventional near-infrared selection.

Taking advantage of the high efficiency of our method, we have been able to trace Sgr tidal debris at Galactic latitudes as low as $|b| \sim 9^{\circ}$. We have followed our WISE \cap 2MASS M giant candidates spectroscopically with AAOmega at the AAT, and show that the identification success rate is as high as 80%. Using bona fide M giant tracers, we provide a new kinematic detection of the Sgr trailing tail debris at $\tilde{\lambda}_{\odot} = 204^{\circ}$. Before crossing the Galactic disk, the trailing tail appears to be moving faster than forecasted by the model of Law & Majewski (2010), in agreement with the prediction of Belokurov et al. (2014).

Our measurement carries important implications for both the disruption of the Sgr dwarf and the Galactic potential: there is now very little doubt that the distant tidal debris discovered in the Northern hemisphere (see, e.g., Drake et al. 2013; Belokurov et al. 2014) is indeed the continuation of the Sgr trailing tail. Such behavior of the trailing tail implies low differential orbital precession of the Sgr stream, which in turn could require diminished dark matter content within 100 kpc (see Gibbons et al. 2014).

ACKNOWLEDGMENTS

The research leading to these results has received funding from the European Research Council under the European Union’s Seventh Framework Programme (FP/2007-2013) / ERC Grant Agreement n. 308024. VB acknowledges financial support from the Royal Society. SK acknowledges financial support from the STFC and the ERC. EO acknowledges support from NSF grant AST-1313006. DBZ acknowledges the financial support of the Australian Research Council. This work has made use of the Q3C open source plugin for PostgreSQL database (Koposov & Bartunov 2006), Astropy software (Astropy Collaboration et al. 2013), Matplotlib software (Hunter 2007). We also thank the anonymous referee for comments which helped us to improve the paper.

REFERENCES

- Astropy Collaboration, Robitaille, T. P., Tollerud, E. J., et al. 2013, *A&A*, 558, A33
- Belokurov, V., Zucker, D. B., Evans, N. W., et al. 2006, *ApJ*, 642, L137
- Belokurov, V., Koposov, S. E., Evans, N. W., et al. 2014, *MNRAS*, 437, 116
- Bessell, M. S., & Brett, J. M. 1988, *PASP*, 100, 1134
- Bressan, A., Marigo, P., Girardi, L., et al. 2012, *MNRAS*, 427, 127
- Correnti, M., Bellazzini, M., Ibata, R. A., Ferraro, F. R., & Varghese, A. 2010, *ApJ*, 721, 329
- Deason, A. J., Belokurov, V., Hamren, K. M., et al. 2014, *arXiv:1407.4458*
- Dohm-Palmer, R. C., Helmi, A., Morrison, H., et al. 2001, *ApJ*, 555, L37
- Drake, A. J., Catelan, M., Djorgovski, S. G., et al. 2013, *ApJ*, 765, 154
- Gibbons, S. L. J., Belokurov, V., & Evans, N. W. 2014, *arXiv:1406.2243*
- Helmi, A., Cooper, A. P., White, S. D. M., et al. 2011, *ApJ*, 733, L7
- Hunter, J.D., 2007, *Computing in Science & Engineering*, 9, 3, 90
- Husser, T.-O., Wende-von Berg, S., Dreizler, S., et al. 2013, *A&A*, 553, A6
- Ibata, R. A., Gilmore, G., & Irwin, M. J. 1994, *Nature*, 370, 194
- Ibata, R., Lewis, G. F., Irwin, M., Totten, E., & Quinn, T. 2001, *ApJ*, 551, 294
- Ibata, R. A., Lewis, G. F., Irwin, M. J., & Cambr esy, L. 2002, *MNRAS*, 332, 921
- Ivezi c,  ., Goldston, J., Finlator, K., et al. 2000, *AJ*, 120, 963
- Koposov, S., & Bartunov, O. 2006, *Astronomical Data Analysis Software and Systems XV*, 351, 735
- Koposov, S. E., Gilmore, G., Walker, M. G., et al. 2011, *ApJ*, 736, 146

- Koposov, S. E., Belokurov, V., Evans, N. W., et al. 2012, *ApJ*, 750, 80
- Koposov, S. E., Belokurov, V., & Wyn Evans, N. 2013, *ApJ*, 766, 79
- Law, D. R., & Majewski, S. R. 2010, *ApJ*, 714, 229
- Lawrence, A., Warren, S. J., Almaini, O., et al. 2007, *MNRAS*, 379, 1599
- Meyer, M. R., Edwards, S., Hinkle, K. H., & Strom, S. E. 1998, *ApJ*, 508, 397
- Majewski, S. R., Siegel, M. H., Kunkel, W. E., et al. 1999, *AJ*, 118, 1709
- Majewski, S. R., Skrutskie, M. F., Weinberg, M. D., & Ostheimer, J. C. 2003, *ApJ*, 599, 1082
- Martínez-Delgado, D., Aparicio, A., Gómez-Flechoso, M. Á., & Carrera, R. 2001, *ApJ*, 549, L199
- Mateo, M., Mirabal, N., Udalski, A., et al. 1996, *ApJ*, 458, L13
- Mateo, M., Olszewski, E. W., & Morrison, H. L. 1998, *ApJ*, 508, L55
- Newberg, H. J., Yanny, B., Rockosi, C., et al. 2002, *ApJ*, 569, 245
- Newberg, H. J., Yanny, B., Grebel, E. K., et al. 2003, *ApJ*, 596, L191
- Niederste-Ostholt, M., Belokurov, V., Evans, N. W., & Peñarrubia, J. 2010, *ApJ*, 712, 516
- Peñarrubia, J., Belokurov, V., Evans, N. W., et al. 2010, *MNRAS*, 408, L26
- Peñarrubia, J., Zucker, D. B., Irwin, M. J., et al. 2011, *ApJ*, 727, L2
- Pietrukowicz, P., Udalski, A., Soszyński, I., et al. 2012, *ApJ*, 750, 169
- Rocha-Pinto, H. J., Majewski, S. R., Skrutskie, M. F., Crane, J. D., & Patterson, R. J. 2004, *ApJ*, 615, 732
- Ruhland, C., Bell, E. F., Rix, H.-W., & Xue, X.-X. 2011, *ApJ*, 731, 119
- Schlegel, D. J., Finkbeiner, D. P., & Davis, M. 1998, *ApJ*, 500, 525
- Sheffield, A., Johnston, K., Majewski, S., et al. 2014, [arXiv:1407.4463](https://arxiv.org/abs/1407.4463)
- Skrutskie, M. F., Cutri, R. M., Stiening, R., et al. 2006, *AJ*, 131, 1163
- Totten, E. J., & Irwin, M. J. 1998, *MNRAS*, 294, 1
- Vivas, A. K., Zinn, R., Andrews, P., et al. 2001, *ApJ*, 554, L33
- Wright, E. L., Eisenhardt, P. R. M., Mainzer, A. K., et al. 2010, *AJ*, 140, 1868
- Yanny, B., Newberg, H. J., Kent, S., et al. 2000, *ApJ*, 540, 825
- Yanny, B., Newberg, H. J., Johnson, J. A., et al. 2009, *ApJ*, 700, 1282
- Wright, E. L., Eisenhardt, P. R. M., Mainzer, A. K., et al. 2010, *AJ*, 140, 1868